ЖУРНАЛ СТРУКТУРНОЙ ХИМИИ

2009. Том 50, № 3 *Май – июнь* *С. 433 – 442*

UDC 539.19

MOLECULAR STRUCTURE, VIBRATIONAL SPECTRA AND POTENTIAL ENERGY DISTRIBUTION OF PROTOPINE USING *AB INITIO* AND DENSITY FUNCTIONAL THEORY

© 2009 **S.A. Siddiqui[1], A. Dwivedi[1], P.K. Singh[1], T. Hasan[1], S. Jain[2], O. Prasad[2], N. Misra[1]***

[1]*Department of Physics, Lucknow University, 226007 India*
[2]*Department of Chemistry, Lucknow University, 226007 India*

Received July, 3, 2008

This work is devoted to theoretical study on molecular structure of protopine. The equilibrium geometry, harmonic vibrational frequencies and infrared intensities were calculated by *ab initio* Hartree-Fock and density functional B3LYP methods with the 6-31G(*d*) basis set and were interpreted in terms of potential energy distribution (PED) analysis. The internal coordinates were optimized repeatedly for many times to maximize the PED contributions. A detailed interpretation of the infrared spectra of protopine is reported. The calculations are in agreement with experiment. The thermodynamic functions of the title compound were also performed at HF/6-31G(*d*) and B3LYP/6-31G(*d*) level of theory. The FT-IR spectra of protopine were recorded in solid phase.

K e y w o r d s: FT-IR spectra, PED, protopine, molecular structure, vibrational spectra.

Protopine is an isoquinoline alkaloid purified from the Chinese medicinal herb, Corydalis Tubers [1]. In folk medicine, the herb or its extract has been traditionally used to treat cardiovascular diseases such as hypertension, cardiac arrhythmia and thromboembolism. Recent experimental studies have shown that the active ingredient from this herb, protopine, significantly reduces blood pressure in dog [2] and the incidence of experimental arrhythmias in a variety of animal models [3, 4]. Protopine from Corydalis Tubers has been shown to have multiple actions on cardiovascular system, including anti-arrhythmic, anti-hypertensive and negative inotropic effects. Although it was thought that protopine exerts its actions through blocking Ca^{2+} currents, the electrophysiological profile of protopine is unclear [5]. Moreover, protopine is able to relax smooth muscles of intestines and vessels [6], inhibit the spastic contraction of isolated guinea-pig ileum induced by acetylcholine and barium chloride, and antagonize the contractile effect of physostigmine-acetylcholine on cat ciliary muscle [7]. In isolated papillary muscle preparations, protopine regulates negatively cardiac contraction and shortens the action potential duration [8]. More recently, Ko *et al.* (1992) suggested that protopine acts as a Ca^{2+} channel antagonist, based on an observation that protopine inhibits the high-potassium induced, Ca^{2+}-dependent contraction of rat aorta [9]. Protopine inhibited acetylcholinesterase activity in a dose-dependent manner. The anti-acetylcholinesterase activity of protopine was specific, reversible and competitive in manner. Furthermore, when mice were pretreated with protopine, the alkaloid significantly alleviated scopolamine-induced memory impairment. In fact, protopine had an efficacy almost identical to that of velnacrine, a tacrine derivative developed by a major drug manufacturer to treat Alzheimer′s disease, at an identical therapeutic concentration. Therefore, protopine has both anti-acetylcholinesterase and antiamnesic properties that may ultimately hold significant therapeutic value in alleviating certain memory impairments observed in dementia [10].

* E-mail: neerajmisralu@rediffmail.com

In the present communication, the experimental FT-IR frequencies of the title molecule are compared with theoretical frequencies obtained by *ab initio* Hartree-Fock and density functional B3LYP methods. To gain a better understanding of the performance and limitation of HF and DFT methods, as a general approach to the vibrational problems of organic molecules, we calculated harmonic frequencies of protopine by HF and DFT methods and compared these results with observed fundamental vibrational frequencies. Thus the comparison of the two methods is useful for obtaining a reliable assignment of the vibrational spectra. The purpose of this study is important due to the further work on modifications of protopine, such as oxidation/reduction that would generate new reactive sites in the molecule to generate patentable compounds of biological interest. The aim of this study is to check the performance of *ab initio* Hartree-Fock and density functional B3LYP methods for simulation of IR spectra of the title compound with the use of standard 6-31G(*d*) basis set. To the best of our knowledge, neither the complete vibrational dynamics nor the potential energy distribution analysis for protopine have been reported so far in the literature.

EXPERIMENTAL

The FT-IR Spectra of protopine have been recorded in CsI on a Perkin Elmer 1800 Spectrophotometer. Spectroscopic preparation of the sample were carried out under an atmosphere of prepurified nitrogen. Protopine was isolated from Fumaria vaillantii [11]. The compound was identified by comparison of its IR, MS and NMR spectra with those reported in literature [12—14].

COMPUTATIONAL DETAILS

The entire calculations were performed at Hartree-Fock (HF) and DFT/B3LYP level on a Pentium IV/1.66 GHZ personal computer using Gaussian 03W [15] program package, invoking gradient geometry optimization [16]. Initial geometry generated from standard geometrical parameters was minimized without any constraint in the potential energy surface at Hartree-Fock level, adopting the standard 6-31G(*d*) basis set. This geometry was then re-optimized again at B3LYP level, using basis set 6-31G(*d*) for better description. The optimized structural parameters were used in the vibrational frequency calculations at the HF and DFT/B3LYP level to characterize all stationary points as minima. We have utilized the gradient corrected density functional theory (DFT) [17] with the three-parameter hybrid functional (B3) [18] for the exchange part and the Lee-Yang-Parr (LYP) correlation function [19], accepted as a cost-effective approach, for the computation of molecular structure, vibrational frequencies, and energies of optimized structures. Vibrational frequencies computed at DFT level have been adjudicated to be more reliable than those obtained by the computationally demanding Moller-Plesset perturbation methods. Density functional theory offers electron correlation frequently comparable to second-order Moller-Plesset theory (MP2) [20, 21]. Next, the spectra were analyzed in terms of the P.E.D. contributions by using the VEDA program [22]. Finally, the calculated normal mode vibrational frequencies provide thermodynamic properties also through the principle of statistical mechanics.

RESULTS AND DISCUSSION

Geometry Optimization. The optimized structure parameters of protopine calculated by *ab initio*, HF and DFT, B3LYP level with the 6-31G(*d*) basis set are listed in Table 1; the atom numbering scheme is given in Fig. 1. Experimental values of bond lengths and angles of protopine are taken from literature [23]. For example, the optimized bond lengths of C—O in ring R1 falls in the range 1.353—1.411 Å for HF and 1.372—1.435 Å for B3LYP method which are in good agreement with those of experimental bond lengths [1.375—

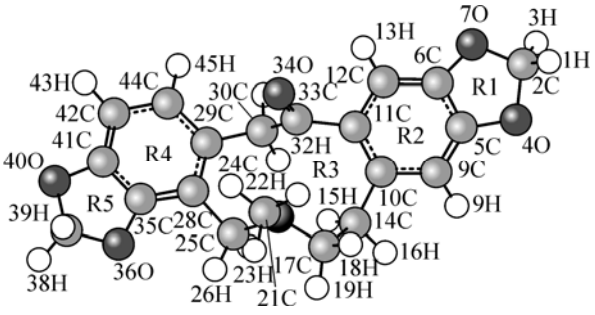

Fig. 1. Model molecular structure of protopine

Table 1

Optimized geometrical parameters of protopine at HF/6-31G(*d*) *and* B3LYP/6-31G(*d*) *levels*

N	Parameter	X-ray	HF	B3LYP	*N*	Parameter	X-ray	HF	B3LYP
1	2	3	4	5	6	7	8	9	10
				Bond lengths (Å)					
1	C2—H1	1.010	1.079	1.094	26	C21—H23	1.040	1.093	1.105
2	C2—H3	1.060	1.082	1.099	27	C21—H24	1.010	1.081	1.093
3	C2—O4	1.428	1.411	1.435	28	C25—H26	1.000	1.089	1.103
4	C2—O7	1.431	1.407	1.430	29	C25—H27	1.050	1.085	1.097
5	O4—C5	1.375	1.353	1.372	30	C25—C28	1.509	1.512	1.512
6	C5—C6	1.376	1.377	1.390	31	C28—C29	1.409	1.414	1.421
7	C5—C8	1.366	1.363	1.378	32	C28—C35	1.371	1.366	1.382
8	C6—O7	1.382	1.359	1.377	33	C29—C30	1.504	1.513	1.512
9	C6—C12	1.363	1.360	1.374	34	C29—C44	1.391	1.379	1.395
10	C8—H9	1.010	1.073	1.085	35	C30—H31	1.000	1.088	1.100
11	C8—C10	1.414	1.408	1.415	36	C30—H32	1.000	1.079	1.092
12	C10—C11	1.398	1.398	1.415	37	C30—C33	1.520	1.524	1.538
13	C10—C14	1.519	1.523	1.519	38	C33=O34	1.218	1.195	1.222
14	C11—C12	1.418	1.410	1.418	39	C35—O36	1.382	1.363	1.381
15	C11—C33	1.505	1.513	1.514	40	C35—C41	1.385	1.382	1.393
16	C12—H13	1.020	1.072	1.083	41	C37—O36	1.421	1.407	1.431
17	C14—H15	1.040	1.083	1.096	42	C37—H38	1.010	1.084	1.093
18	C14—H16	1.020	1.085	1.096	43	C37—H39	1.030	1.078	1.100
19	C14—C17	1.525	1.534	1.544	44	C37—O40	1.419	1.406	1.430
20	C17—H18	1.030	1.083	1.095	45	C41—O40	1.385	1.359	1.378
21	C17—H19	1.050	1.092	1.105	46	C41—C42	1.363	1.361	1.378
22	C17—N20	1.461	1.450	1.460	47	C42—H43	1.020	1.073	1.084
23	N20—C21	1.458	1.450	1.458	48	C42—C44	1.398	1.402	1.407
24	N20—C25	1.466	1.455	1.467	49	C44—H45	1.000	1.075	1.086
25	C21—H22	1.040	1.082	1.093					
				Bond angles (deg.)					
50	H1—C2—H3	119.7	110.9	110.9	94	H22—C21—H23	109.3	108.8	108.9
51	H1—C2—O4	107.8	109.5	109.3	95	H22—C21—H24		107.6	107.6
52	H1—C2—O7		109.7	109.5	96	H23—C21—H24	107.8	108.5	108.7
53	H3—C2—O4		109.4	109.3	97	N20—C25—H26	112.5	111.4	111.3
54	H3—C2—O7	104.1	109.8	109.6	98	N20—C25—H27		108.4	107.7
55	O4—C2—O7	108.2	107.5	108.2	99	N20—C25—C28	110.3	112.3	112.5
56	C2—O4—C5	105.7	106.5	105.6	100	H26—C25—H27	105.5	106.3	106.3
57	O4—C5—C6	109.7	109.4	109.9	101	H26—C25—C28		109.6	109.8
58	O4—C5—C8	128.1	129.0	128.5	102	H27—C25—C28	108.8	108.6	109.0
59	C6—C5—C8	122.2	121.6	121.5	103	C25—C28—C29	120.3	122.1	122.0
60	C5—C6—O7	110.2	109.2	109.7	104	C25—C28—C35	123.5	121.7	121.8
61	C5—C6—C12	121.7	121.2	121.3	105	C29—C28—C35	116.2	116.1	116.2
62	O7—C6—C12	128.1	129.5	129.0	106	C28—C29—C30	118.7	119.8	119.6
63	C2—O7—C6	105.1	106.5	105.7	107	C28—C29—C44	120.8	120.2	120.2
64	C5—C8—H9	119.2	120.2	120.4	108	C30—C29—C44	120.5	119.9	120.2
65	C5—C8—C10	118.1	119.0	119.0	109	C29—C30—H31	110.1	109.2	109.2
66	H9—C8—C10	122.7	120.8	120.6	110	C29—C30—H32		111.3	111.7

Table 1 (continued)

1	2	3	4	5	6	7	8	9	10
67	C8—C10—C11	119.6	119.0	119.2	111	C29—C30—C33	113.6	114.1	113.8
68	C8—C10—C14	115.9	115.4	116.0	112	H31—C30—H32	109.0	105.7	105.7
69	C11—C10—C14	124.4	125.5	124.5	113	H31—C30—C33		104.6	104.8
70	C10—C11—C12	120.7	120.5	120.4	114	H32—C30—C33	110.1	111.3	111.0
71	C10—C11—C33	127.0	127.0	126.9	115	C11—C33—C30	117.2	119.6	119.2
72	C12—C11—C33	112.3	112.4	112.6	116	C11—C33=O34	119.9	119.3	119.6
73	C6—C12—C11	117.8	118.5	118.5	117	C30—C33=O34	120.8	120.0	119.7
74	C6—C12—H13	125.2	121.5	121.9	118	C28—C35—O36	127.8	128.1	127.6
75	C11—C12—H13	117.0	120.0	119.6	119	C28—C35—C41	122.5	123.2	123.0
76	C10—C14—H15	110.8	111.5	112.0	120	C41—C35—O36	109.7	108.8	109.3
77	C10—C14—H16		107.8	108.4	121	C35—O36—C37	105.8	106.5	105.2
78	C10—C14—C17	113.9	114.0	113.3	122	O36—C37—H38	112.1	109.6	109.4
79	H15—C14—H16	103.6	105.4	105.5	123	O36—C37—H39		109.6	109.5
80	H15—C14—C17		109.9	109.2	124	O36—C37—O40	109.1	107.4	108.0
81	H16—C14—C17	110.7	107.9	108.0	125	H38—C37—H39	106.0	110.8	111.0
82	C14—C17—H18	112.1	108.4	108.6	126	H38—C37—O40	107.0	109.7	109.5
83	C14—C17—H19		109.3	109.5	127	H39—C37—O40		109.6	109.5
84	C14—C17—N20	111.8	112.0	111.7	128	C37—O40—C41	105.8	106.4	105.3
85	H18—C17—H19	108.2	106.6	106.7	129	C35—C41—O40	109.6	109.2	109.7
86	H18—C17—N20		108.7	108.5	130	C35—C41—C42	122.2	121.6	121.5
87	H19—C17—N20	110.1	111.6	111.8	131	O40—C41—C42	128.2	129.2	128.8
88	C17—N20—C21	113.2	113.9	114.7	132	C41—C42—H43	121.9	121.8	121.7
89	C17—N20—C25	112.5	113.0	112.9	133	C41—C42—C44	116.5	116.4	116.4
90	C21—N20—C25	111.0	112.4	112.6	134	H43—C42—C44	121.5	121.8	121.9
91	N20—C21—H22	110.5	109.6	109.5	135	C29—C44—C42	121.8	122.4	122.5
92	N20—C21—H23		112.5	112.8	136	C29—C44—H45	120.7	119.1	118.8
93	N20—C21—H24	111.9	109.6	109.2	137	C42—C44—H45	117.5	118.5	118.7

1.431 Å]; optimized bond lengths of C—O in R5 falls in the range 1.359—1.407 Å for HF and 1.378—1.431 Å for B3LYP method which are also in good agreement with experimental bond lengths [1.382—1.421 Å]. The optimized bond lengths of C—C in ring R2 falls in the range 1.360—1.410 Å for HF and 1.374—1.418 Å for B3LYP method which are also in good agreement with those of experimental bond lengths [1.363—1.418 Å]. The optimized C—C bond lengths in ring R3 falls in the range 1.414—1.534 Å for HF and 1.421—1.544 Å for B3LYP method which are also in excellent agreement with those of experimental bond length [1.371—1.525 Å]. The optimized C—C bond length in ring R4 falls in the range 1.361—1.414 Å for HF and 1.378—1.421 Å for B3LYP method which are also in excellent agreement with those of experimental bond lengths [1.363—1.409 Å]. The optimized C—N bond length falls in the range 1.450—1.455 Å for HF and 1.458—1.467 Å for B3LYP method which are also in excellent agreement with those of experimental bond lengths [1.458—1.466 Å]. The value of optimized C=O bond length is 1.195 Å for HF and 1.222 Å for B3LYP method, which is also in good agreement with experimental bond length 1.218 Å. The other calculated bond lengths and bond angles also are in excellent agreement with the experimental values. Based on the above comparison, although there are some difference between the theoretical values and experimental values, the optimized structural parameters can well reproduce the experimental ones and they are the basis for thereafter discussion.

Vibrational Assignments. The molecule has 45 atoms and 129 normal modes of fundamental vibration. Detailed description of vibrational modes can be given by means of normal coordinate analy-

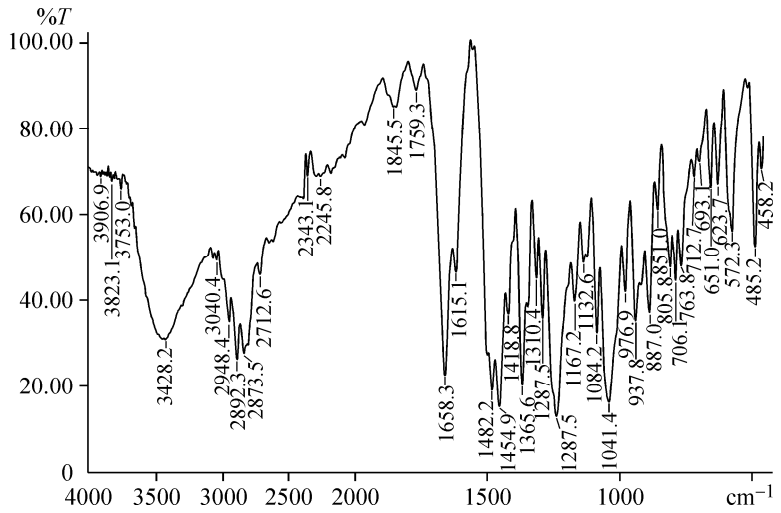

Fig. 2. FT-IR spectra of protopine

sis. The detailed vibrational assignments are achieved by comparing the band positions and intensities observed in FT-IR spectra with wave numbers and intensities from molecular modeling calculations at HF/6-31G(*d*) and B3LYP/6-31G(*d*) level.

The experimental FT-IR spectrum is shown in Fig. 2. Vibrational frequencies calculated at HF/6-31G(*d*) level were scaled by 0.89 and at B3LYP/6-31G(*d*) level were scaled by 0.96 [24]. The descriptions concerning the assignment have also been listed in Table 2. VEDA Program [22] was used for P.E.D. analysis and to assign the calculated harmonic frequencies.

The harmonic vibrational frequencies calculated for protopine at B3LYP level using 6-31G(*d*) have been collected in Table 2. The observed FT-IR frequencies for various modes of vibrations are also presented in Table 2. Several calculated thermodynamic parameters are presented in Table 3. The data related to HF calculations are available from the authors.

Carbonyl Absorption. Carbonyl absorptions are sensitive and both the carbon and oxygen atoms of the carbonyl group move during the vibration and they have nearly equal amplitude. In the present study the C=O stretching vibration is observed at 1658 cm^{-1} and is in agreement with the calculated frequency obtained at 1755 cm^{-1} for HF and at 1685 cm^{-1} for B3LYP method with P.E.D. 92 % and 90 %, respectively.

C—N Vibrations. The identification of C—N vibrations is a difficult task, since the mixing of vibrations is possible in this region. In this study the C—N stretching vibration are observed at 786 and 1041 cm^{-1}, and it is calculated at 802 and 1036 cm^{-1} for HF, and at 790 and 1025 cm^{-1} for B3LYP method with P.E.D. 29 % and 54 %, and 27 % and 55 %, respectively. The various bending and torsional vibrations assigned in this study are also supported by the literature [25].

C—H Vibrations. The hetero aromatic structure shows the presence of C—H stretching vibrations in the region 3000—3100 cm^{-1} which is the characteristic region for the ready identification of the C—H stretching vibration [26]. In the present study the C—H stretching vibrations of the title compound are observed at 3070, 3040, 2837 and 2713 cm^{-1} which are in good agreement with the calculated frequencies at 3048, 3029, 2838 and 2800 cm^{-1} for HF and at 3114, 3099, 2870 and 2849 cm^{-1} for B3LYP method with high percentage of P.E.D. The various bending vibrations assigned in this study are also supported by the literature [26].

Methylene Group Vibrations. The antisymmetric CH_2 stretching vibrations are generally observed in the region 3100—3000 cm^{-1}, while the symmetric stretching vibrations are generally observed in the region 3000—2900 cm^{-1} [27]. For Hartree-Fock method, the CH_2 antisymmetric stretching vibrations are calculated at 2962, 2958, 2952, 2911 and 2900 cm^{-1}, whereas CH_2 symmetric stretching vibrations are calculated at 2897, 2888, 2885, 2878, and 2858 cm^{-1}, respectively with high

T a b l e 2

Vibrational wave numbers obtained for protopine at B3LYP/6-31G(*d*) *in* cm^{-1}, *experimental frequencies from* FT-IR *spectra in* cm^{-1}, IR *intensities* (K_m, mol^{-1}), *and assignment with* P.E.D. *percentage in square brackets*

N	Wave Number		Exp. Freq.	IR Int.	Assignment [P.E.D]
	Unscal.	Scal.	I R		
1	2	3	4	5	6
1	29	27		1	τ(CCCC)R4[50]+ϕ(CCC)R3[31]
2	52	50		1	τ(COCO)R1[72]
3	61	58		0	τ(CCCC)R3[68]
4	68	65		6	τ(COCO)R1[83]
5	91	87		4	τ(COCO)R5[65]
6	96	92		1	τ(CCCC)R2&R3[71]
7	104	100		1	τ(COCO)R5[67]
8	115	111		5	τ(COCO)R5[64]
9	154	148		2	ϕ(CCO)R1&R2[20]+τ(CCNC)R3[11]+ϕ(CCC)R2&R3[10]
10	158	152		1	τ(CCNC)R3[54]
11	168	161		1	τ(CCCC)R4[15]
12	197	189		2	τ(CCCC)R4[45]+ϕ(CCO)R2&R1[20]
13	210	202		0	τ(HCNC)adj R3[78]
14	229	220		4	τ(CCCO)R2&R1[31]+ϕ(CCC)R2&R3[24]+ϕ(CCC)R3[11]
15	247	237		1	τ(OCCC)R1&R2[14]+ϕ(CCC)R3[11]+τ(CCCO)R2&R1[10]
16	270	259		0	τ(CNCC)R3[47]
17	283	272		2	τ(CCCO)R2&R1[20]+τ(CCC=O)[11]+ϕ(CCC)R3[10]
18	298	286		1	τ(CCCO)R4&R5[64]
19	324	311		6	ϕ(CNC)R3[26]
20	347	333		2	ϕ(CNC)R3[29]+τ(OCCC)R1&R2[14]
21	363	348		1	τ(CCCO)R3,R4&R5[50]
22	374	359		1	ϕ(CCO)R2&R1[42]
23	389	374		1	ϕ(CCC)R3[13]
24	398	382		0	τ(OCCC)R1&R2[44]+ϕ(CNC)R3[10]
25	434	416		4	ϕ(CNC)adj R3[46]
26	441	423		3	τ(O=CCC)[59]
27	467	449		6	ϕ(CC=O)[40]
28	483	463	458	0	ϕ(CCN)[53]
29	488	469		17	ϕ(CCC)R4[51]
30	500	480	485	8	ϕ(CCC)R4[52]
31	520	499	530	2	τ(CCCC)R4[43]
32	585	561		13	τ(CCC=O)R2&R3[29]+ϕ(CCC)R3[17]
33	597	573	572	15	τ(CCCC)R4[28]+ϕ(CCO)R4&R5[10]
34	611	587		0	ϕ(CCC)R3[32]
35	631	605	624	6	ϕ(CCO)R4&R5[30]+τ(CCCC)R4[12]
36	665	638	651	10	ϕ(CC=O)[43]
37	683	656		0	τ(OCCC)R1&R2[78]
38	702	674		6	τ(CCCO)R3,R4&R5[38]+ν(CC)R4[13]
39	722	693		0	τ(CCCC)R2[30]+τ(CCCO)R3,R4&R5[10]
40	730	701	693	4	ϕ(COC)R1[59]

Table 2 (continued)

1	2	3	4	5	6
41	739	709	713	0	τ(CCCC)R2[19]+τ(CCCO)R3,R4&R5[15]+ϕ(COC)R5[10]
42	752	722		3	ϕ(COC)R1[52]+ν(CC)R3[15]
43	772	741		4	ν(CC)R4[37]+ϕ(COC)R5[37]
44	779	748		6	ϕ(CCC)R4[27]
45	802	770	764	26	τ(HCCC)R4[45]+ν(NC)R3[12]
46	822	790	786	23	ν(NC)R3[27]+τ(HCCC)R4[22]
47	841	807	806	16	ν(OC)R1[27]+ϕ(CC=O)[14]+τ(HCCC)R4[13]
48	865	831	851	17	ν(OC)R1[12]
49	868	833		9	τ(HCCO)R2&R1[89]
50	889	853		22	τ(CCCH)R2[78]
51	917	880		0	τ(HCCH)R4[64]+ν(OC)R5[10]
52	920	883	887	6	ν(OC)R5[32]+τ(HCCH)R4[21]
53	936	898		2	ν(CC)R3[42]
54	943	906	910	12	τ(CCCH)R3[37]
55	949	911		6	τ(CCCH)R3[37]
56	977	938	938	7	ν(OC)R5[69]
57	978	939		63	ν(OC)R1[71]
58	995	956	977	38	ν(CC)R3[41]
59	1035	993		20	τ(CCNH)R3[28]+ν(OC)R5[13]+ν(OC)R5[11]
60	1038	997		17	ν(OC)R5[51]
61	1057	1015		4	τ(CCNH)[37]+ν(NC)adj R3[11]
62	1067	1025	1041	33	ν(NC)R3[55]+τ(CHNH)[13]
63	1076	1033		219	ν(OC)R1[77]
64	1094	1050		143	ν(OC)R5[68]
65	1104	1060		81	ν(OC)R1[58]
66	1152	1106	1084	12	ϕ(HCO)R1[94]
67	1154	1108		3	ϕ(HCC)R3[46]+ν(CC)R4[14]
68	1157	1111		13	ϕ(HCO)R5[82]
69	1161	1115	1115	14	ϕ(HCN)[60]
70	1165	1118		15	ϕ(HCC)R3[38]+ν(NC)adj R3[18]
71	1184	1137	1133	9	ϕ(HCC)R3[47]+ν(CC)R3[11]
72	1190	1143		5	ϕ(HCC)R2[29]+ν(CC)R3[25]
73	1204	1155		35	ϕ(HCO)R1[25]
74	1210	1161		1	ϕ(HCO)R1[84]
75	1216	1167	1167	2	ϕ(HCO)R5[78]
76	1222	1173		17	ϕ(HCC)R2[17]
77	1231	1182		4	ν(CC)R3[39]+ϕ(HCO)R5[10]
78	1259	1209		13	τ(CHNH)[29]+ϕ(HCN)[10]
79	1277	1225		12	ν(CC)R3&R4[48]
80	1282	1230		348	ν(CC)R2[47]
81	1296	1244	1237	232	ϕ(HCC)R4[38]+ν(CC)R3[10]+ν(CC)R4[10]
82	1304	1251		32	ϕ(HCC)R2[46]+ν(CC)R2[12]
83	1320	1267		2	ϕ(HCN)[56]
84	1343	1290	1287	66	ϕ(HCO)R1[17]+τ(CCNH)[14]+ϕ(HCC)R3[11]
85	1353	1298		28	ϕ(HCC)R3[60]
86	1381	1326	1310	37	ϕ(HCC)R3[67]

Table 2 (continued)

1	2	3	4	5	6
87	1405	1349		47	ν(CC)R2[59]
88	1409	1353	1366	51	ν(CC)R4[57]
89	1414	1357		69	ϕ(HCN)[59]
90	1421	1364		24	ϕ(HCC)R3[73]
91	1435	1378		8	ν(CC)R2[33]+τ(CHOH)R1[25]
92	1452	1394		8	τ(CHOH)R5[77]
93	1461	1403	1419	5	τ(CHOH)R1[51]+ν(CC)R2[17]
94	1483	1424		3	ϕ(HCH)adj N[86]
95	1497	1438		29	ϕ(HCH)R3[75]
96	1503	1443	1455	166	ν(CC)R4[51]+ϕ(HCC)R3[12]
97	1514	1454		7	ϕ(HCH)adj N[84]
98	1520	1459		100	ν(CC)R4[52]+ϕ(HCC)R4[20]
99	1521	1461		4	ϕ(HCH)R3[76]
100	1525	1464		4	ϕ(HCH)R3[83]
101	1533	1471		76	ϕ(HCH)R3[71]
102	1535	1474		9	ϕ(HCH)R3[80]
103	1539	1477	1482	279	ν(CC)R1&R2[40]+ϕ(HCC)R3[10]
104	1572	1509		2	ϕ(HCH)R5[94]
105	1577	1514		1	ϕ(HCH)R1[89]
106	1660	1594	1560	4	ν(CC)R2[73]
107	1661	1595		5	ν(CC)R4[62]
108	1670	1603	1615	30	ν(CC)R2[66]
109	1694	1626		1	ν(CC)R4[72]
110	1755	1685	1658	123	ν(C=O)[90]
111	2960	2841		36	ν(CH)R3[90]
112	2967	2849	2713	130	ν(CH)R3[88]
113	2989	2870	2837	73	ν(CH)R3[93]
114	3018	2897	2892	145	$\nu_s(CH_2)$R5[94]
115	3034	2913		159	$\nu_s(CH_2)$R1[100]
116	3038	2917		19	$\nu_s(CH_2)$R3[95]
117	3057	2935		18	$\nu_s(CH_2)$R3[91]
118	3064	2941		34	$\nu_s(CH_2)$R3[86]
119	3085	2962		21	$\nu_{as}(CH_2)$R3[93]
120	3101	2976		33	$\nu_{as}(CH_2)$R3[79]
121	3107	2983		20	$\nu_s(CH_3)$adj N[86]
122	3109	2985	2948	57	$\nu_{as}(CH_2)$R1[100]
123	3121	2996		59	$\nu_{as}(CH_2)$R5[94]
124	3125	3000		19	$\nu_{as}(CH_2)$R3[92]
125	3149	3023		17	$\nu_{as}(CH_3)$adj N[99]
126	3196	3068		10	ν(CH)R4[95]
127	3212	3084		7	ν(CH)R2[99]
128	3228	3099	3040	8	ν(CH)R4[95]
129	3244	3114	3070	2	ν(CH)R2[100]

Note: Abbreviations used here have the following meaning: ν, stretching; ν_s, symmetric stretching; ν_{as}, asymmetric stretching; ϕ, bending; τ, torsion; R, ring; adj, adjacent.

Table 3

Theoretically computed energies (a.u), *zero-point vibrational energies* (kcal·mol^{-1}), *rotational constants* (GHz), *entropies* (Cal·mol^{-1}·K^{-1}) *and dipole moment* (*D*) *for protopine at* HF *and* B3LYP *levels of theory*

Parameter	HF/6-31G(*d*)	B3LYP/6-31G(*d*)	Parameter	HF/6-31G(*d*)	B3LYP/6-31G(*d*)
Total energy	–1197.13468972	–1204.37974417	Entropy		
Zero-point energy	245.22353	227.48358	Total	146.464	151.253
Rotational Constants	0.62398	0.61539	Translational	43.479	43.479
	0.10114	0.10026	Rotational	35.263	35.290
	0.09259	0.09219	Vibrational	67.723	72.484
			Dipole moment	3.539	2.808

percentage of P.E.D. For B3LYP method, the CH_2 antisymmetric stretching vibrations are calculated at 3000, 2996, 2985, 2976 and 2962 cm^{-1}, whereas CH_2 symmetric stretching vibrations are calculated at 2941, 2935, 2917, 2913 and 2897 cm^{-1}, respectively with high percentage of P.E.D. The bands corresponding to different bending vibrations of CH_2 group are summarized in Table 2 and are also supported by the literature [27].

Methyl group vibrations. The CH_3 symmetric stretching vibration is calculated at 2916 cm^{-1} and the CH_3 antisymmetric stretching vibration is calculated at 2963 cm^{-1} with P.E.D. 85 % and 98 %, respectively, for HF method, whereas CH_3 symmetric stretching vibration is calculated at 2983 cm^{-1} and the CH_3 antisymmetric stretching vibration is calculated at 3023 cm^{-1} with P.E.D. 86 % and 99 %, respectively, for B3LYP method. These assignments are also supported by the literature [28]. In the present study various bending vibrations of CH_3 group are summarized in Table 2 and are also supported by the literature [28].

CC Ring Vibrations. The C—C aromatic stretch known as semi-circle stretching, calculated at 1624, 1605, 1495, 1450, 1353 and 997 cm^{-1} for HF method with appropriate P.E.D., are in perfect agreement with the observed frequencies. For B3LYP method these are calculated at 1603, 1594, 1477, 1443, 1353 and 956 cm^{-1}; they are also in good agreement with observed frequencies with appropriate P.E.D. The theoretically calculated C—C—C bending and C—C torsional modes have been found to be consistent with the recorded spectral values.

CO Ring vibrations. In this study the C—O stretching vibrations are calculated at 1067, 1061, 1051, 1018, 987, 960, 906, 846 and 820 cm^{-1} for HF method with significant percentage of P.E.D., whereas for B3LYP method C—O stretching vibrations are calculated at 1060, 1050, 1033, 997, 939, 938, 883, 831 and 807 cm^{-1}, respectively, with appropriate P.E.D.; they are also supported by the literature [29], as well as various bending and torsional vibrations assigned in this study [29].

Other molecular properties. Several calculated thermodynamic properties at HF and B3LYP level are listed in Table 3. In this study total energy is greater for B3LYP method, while zero point energy is greater for HF method. Values of all rotational constants and dipole moment are also greater for HF method, while entropy is greater for B3LYP method. These thermodynamic parameters clearly indicate that vibration motion play a crucial role in order to access the thermodynamic behavior of the title compound.

CONCLUSION

The equilibrium geometries and harmonic frequencies of protopine were determined and analyzed at both HF and DFT levels of theory. The vibrational frequency calculation proved that the structure is stable (no imaginary frequencies). The difference between the observed and scaled wave number values of most of the fundamentals is very small. Any discrepancy noted between the observed and the calculated frequencies may be due to the fact that the calculations have been actually done on a single molecule in the gaseous state contrary to the experimental values recorded in the presence of intermolecular interactions. The potential energy distribution contribution to each of the observed frequencies shows the reliability and accuracy of the normal mode analysis. The normal mode analysis of pro-

topine shows a dynamical behavior and, possibly, opens up an avenue for further conformational research. With the continuing need for novel structures and the difficulty of gaining access to large tracts of biodiversity in habitats, combinatorial chemistry blended with modern quantum chemical methods can prove to be extremely useful for the researchers.

Acknowledgement. The authors wish to acknowledge the Muslim Association for the Advancement of Science ″MAAS″, Aligarh, for providing financial support.

REFERENCES

1. *Jiang B., Cao K., Wang R.* // Eur. J. Pharmacol. – 2004. – **506**. – P. 93 – 100.
2. *Wang D.Y., Cheng M.Z., Wang C.G. et al.* // Chin. J. Integr. Trad. Wes. Med. – 1986. – **6**. – P. 477 – 479.
3. *Burtsev V.N., Dormidontov E.N., Saliaev V.N.* // Kardiologiia. – 1978. – **18**. – P. 76 – 79.
4. *Lu Z.A., Wan D.C., Chen Z.H., Wang X.H.* // Chin. Pharmaceut. J. – 1992. – **30**. – P. 81 – 84.
5. *Song L.S., Ren G.J., Chen Z.L. et al.* // Brit. J. Pharmacology. – 2000. – **129**. – P. 893 – 900.
6. *Huang Y.H., Zhang Z.Z., Jiang J.X.* // Acta Pharmacol. Sinica. – 1991. – **12**. – P. 16 – 19.
7. *Zhong R.X., Shi R.R., Huang L.X. et al.* // Chin. Trad. Herb. Drugs. – 1986. – **17**. – P. 303 – 306.
8. *Teng C.X., Chen Z.H., Zhao G.S.* // Acad. J. Kunming Med. Coll. – 1989. – **10**. – P. 44 – 46.
9. *Ko F.N., Wu T.S., Lu S.T. et al.* // Jpn. J. Pharmacol. – 1992. – **58**. – P. 1 – 9.
10. *Kim S.R., Hwang S.Y., Jang Y.P. et al.* // Planta Medica. – 1999. – **65**. – P. 218 – 221.
11. *Sadikov A.Z., Babaev B., Shakirov T.T.* // Chem. Natur. Compounds. – 1976. – **10**, N 6. – P. 852.
12. *Takahashi H., Iguchi M., Onda M.* // Chem. Pharmaceut. Bull. – 1985. – **33**. – P. 4775 – 4782.
13. *Dolejs L., Slavik J., Hanus V.* // Coll. Czechoslovak Chem. Commun. – 1964. – **29**, N 10. – P. 2479.
14. *Tousek J., Malinakova K., Dostal J., Marek R.* // Magn. Reson. Chem. – 2005. – **43**, N 7. – P. 578 – 581.
15. *Frisch M.J., Trucks G.W., Schlegal H.B. et al.* Gaussian, Inc., Wallingford CT, 2004.
16. *Schlegel H.B.* // J. Comput. Chem. – 1982. – **3**. – P. 214 – 218.
17. *Hohenberg P., Kohn W.* // Phys. Rev. – 1964. – **B136**. – P. 864 – 871.
18. *Becke A.D.* // J. Chem. Phys. – 1993. – **98**. – P. 5648 – 5652.
19. *Lee C., Yang W., Parr R.G.* // Phys. Rev. – 1988. – **B37**. – P. 785 – 789.
20. *Sundaraganesan N., Saleem H., Mohan S., Ramalingam M.* // Spectrochim. Acta. – 2005. – **A61**. – P. 377 – 385.
21. *Sundaraganesn N., Ilakiamani S., Saleem H. et al.* // Ibid. – P. 2995 – 3001.
22. *Jamroz M.H.* Vibrational Energy Distribution Analysis: VEDA 4 Program, Warsaw, 2004.
23. *Hall S.R., Ahmed F.R.* // Acta Crystall. – 1968. – **B24**. – P. 337 – 346.
24. *Fast P.L., Corchado J., Sanches M.L., Truhlar D.G.* // J. Phys. Chem. – 1999. – **A103**. – P. 3139 – 3143.
25. *Krishnakumar V., Xavier R.J.* // Spectrochim. Acta. – 2004. – **A60**. – P. 709 – 714.
26. *Krishnakumar V., Xavier R.J.* // Indian J. Pure Appl. Phys. – 2003. – **41**. – P. 597 – 601.
27. *Krishnakumar V., Xavier R.J., Chithambarathanu T.* // Spectrochim. Acta. – 2005. – **A62**. – P. 931 – 939.
28. *Bunce S.J., Edwards H.G., Johnson A.F. et al.* // Ibid. – 1993. – **A49**. – P. 775 – 783.
29. *Krishnakumar V., Ramasamy R.* // Ibid. – 2005. – **A61**. – P. 673 – 683.